ROYAL SOCIETY OF CHEMISTRY

PERSPECTIVE
Joshua Jack *et al.*
Electrified CO$_2$ valorization in emerging nanotechnologies: a technical analysis of gas feedstock purity and nanomaterials in electrocatalytic and bio-electrocatalytic CO$_2$ conversion

PERSPECTIVE

Check for updates

Electrified CO_2 valorization in emerging nanotechnologies: a technical analysis of gas feedstock purity and nanomaterials in electrocatalytic and bio-electrocatalytic CO_2 conversion†

Joshua Jack, [iD] *[a] Aidan Weber,[c] Sara Bolzman[a] and Stephen McCord[b]

Engineered nanomaterials that catalyze the transformation of waste carbon dioxide (CO_2) into value-added products are crucial to mitigate climate change and enable a new circular carbon economy. Gas separations are expected to be a major cost barrier to CO_2 conversion scalability, but the importance of feedstock purity is yet to be carefully evaluated in emerging nanotechnologies under environmentally relevant conditions. Here we assessed the performance of state-of-the-art electrocatalytic and bio-electrocatalytic CO_2 reduction nanomaterials under a range of influent CO_2 concentrations using data from recent publications. We quantitatively compared the activity of various electrocatalysts and discussed interactions at the nano-bio interface. Through this perspective, we developed initial life-cycle assessments and technoeconomic analyses for the integration of CO_2 conversion nanotechnologies with natural and engineered systems. Altogether this evaluation can inform innovative nanomaterial design and delivers useful insights towards a sustainable future without waste or pollution.

Environmental significance

Breakthroughs in nanomaterial design are needed to minimize wastes, reuse materials, and promote a new circular economy. Though electrocatalytic and bio-electrocatalytic approaches have shown promise for CO_2 upgrading, their performance has largely been demonstrated with high purity gas feedstock that is often not practical or environmentally relevant. As such, new insights are needed to integrate waste CO_2 streams with state-of-the-art nanotechnologies. For the first time, we analyzed the importance of gas purity on nanomaterial activity and design. We discuss potential mechanisms for electrocatalyst inactivation, rate limiting steps at the nano-bio interface, and identify challenges in employing nanomaterials in industrial applications. Altogether, this perspective aims to illuminate new interdisciplinary opportunities to advance carbon circularity and environmental science through next-generation nanoscale processes.

1. Introduction

Rapid decarbonization is imperative to avoid the severe economic and environmental implications of global climate change. Despite the existence of technically feasible CO_2 capture and sequestration methods, the widespread adoption of these technologies has been constrained by the low intrinsic value of CO_2 molecules. To overcome these challenges, current research initiatives have focused on the development of new reactive CO_2 conversion nanotechnologies that can boost the value proposition of carbon cycling by combining cheap and abundant renewable electrons with waste CO_2 to generate value-added products [Fig. 1]. Recently, engineered nanomaterials have been leveraged in diverse CO_2 conversion applications with electrocatalytic and bio-electrocatalytic processes being amongst the most promising. For instance, the electrochemical reduction of CO_2 using copper nanoparticles can produce useful molecules such as CO, HCOOH, C_2H_4, and C_2H_5OH at high production rates.[1] As such, many studies have focused on developing new nanomaterials for the targeted production of fuels and chemicals from CO_2 and have shown excellent titers and efficiencies.[2] In particular, CO has been an attractive product as it is an essential building block for industrial chemical manufacturing and can be produced with high

[a] Department of Civil and Environmental Engineering, University of Michigan, Ann Arbor, MI, 48109, USA. E-mail: jdjack@umich.edu; Tel: +1 (734) 764 0452
[b] Global CO_2 Initiative, University of Michigan, Ann Arbor, MI, 48109, USA
[c] Department of Chemical Engineering, University of Michigan, Ann Arbor, MI, 48109, USA
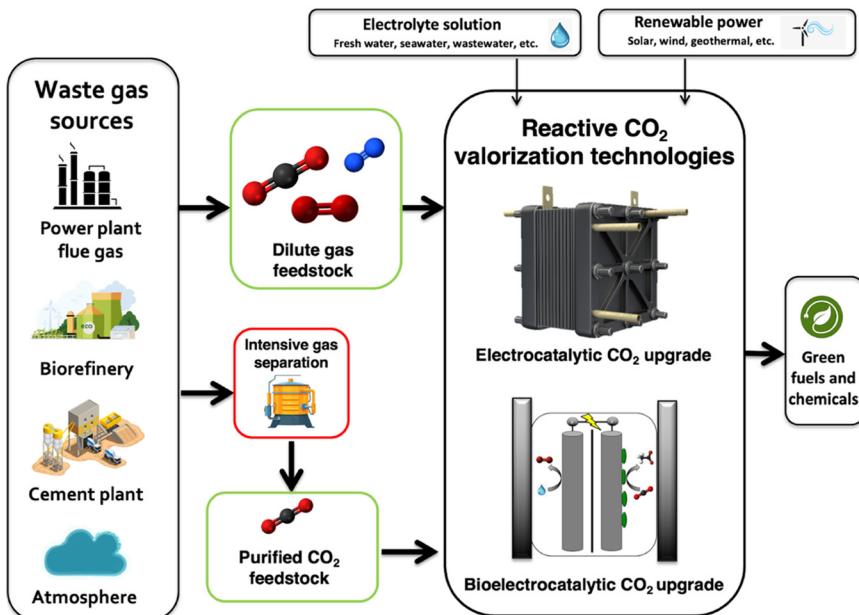
Fig. 1 Overview of emerging CO_2 capture and conversion pathways. Proposed process flow for electrified CO_2 conversion with selection of waste gas feedstock, omission or inclusion of gas separation device, and choice of CO_2 conversion nanotechnology.

selectivity.[3,4] Alongside electrocatalytic approaches, researchers have also been developing new bio-electrocatalytic CO_2 conversion processes such as microbial electrosynthesis (MES) that uses whole-cell bacteria supported on conductive

nanomaterials to generate valuable products from waste CO_2 and renewable energy.[5] Recently, several MES studies have shown exceptional selectivity for energy rich molecules such as acetate.[6] For example, researchers have shown that *Sporomusa*
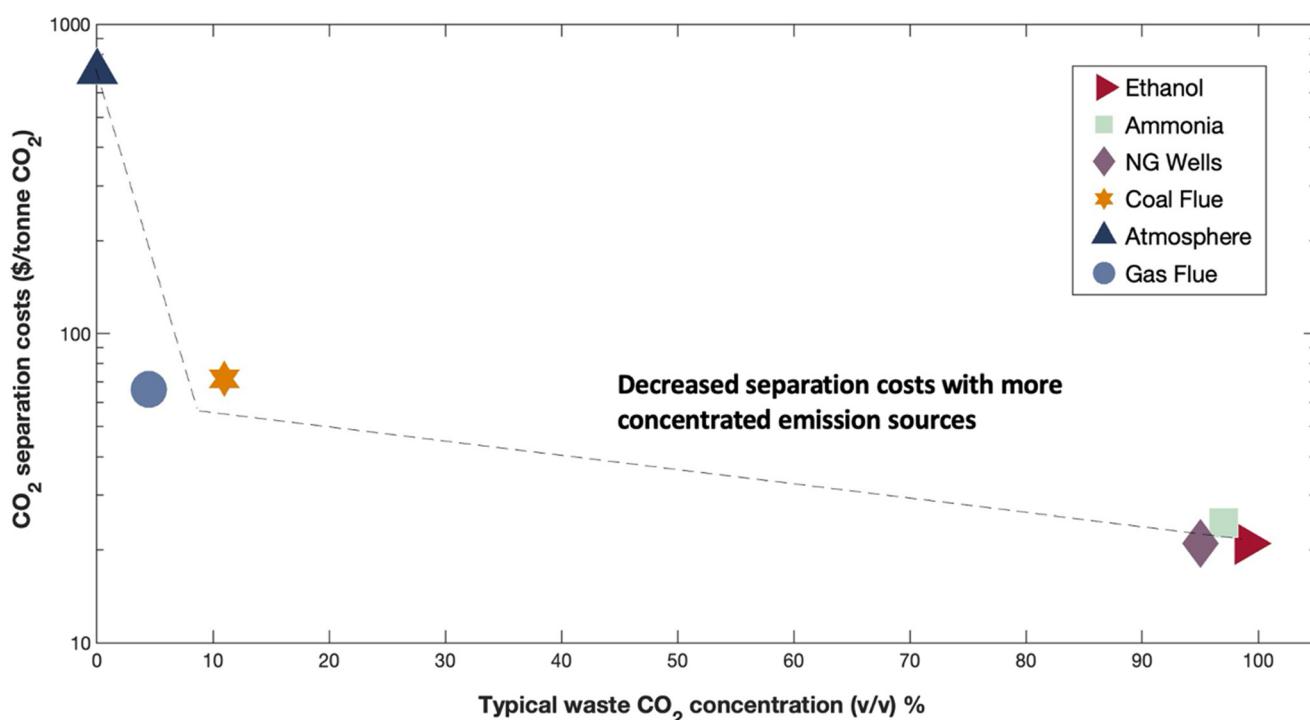
Fig. 2 Estimated CO_2 separation costs across typical industrial point source and non-point source emission concentrations. Expected CO_2 separation costs ($/tonne CO_2) *versus* typical waste CO_2 concentrations % (v/v). Emission sources listed in legend where ethanol = ethanol fermentation, ammonia = ammonia synthesis plant, NG wells = natural gas well, coal flue = coal fired power plant flue gas, atmosphere = ambient air, gas flue = natural gas-powered plant flue gas. Interpolation as dotted line. Data obtained from recent publication ref. 8.

This journal is © The Royal Society of Chemistry 2024

Environ. Sci.: Nano, 2024, **11**, 1770–1783 | **1771**

ovata can achieve exceptional columbic efficiencies (~90%) for acetate biosynthesis when grown on 3D-graphene functionalized carbon felt electrodes.[7]

Though promising, the performance and value proposition of these new CO_2 conversion nanotechnologies are expected to be inherently tied to the source of waste CO_2 feedstock. This source can span the range from the near-infinite but dilute natural atmospheric supply (~415 ppm) to more concentrated but location specific streams released from ammonia synthesis plants or biorefineries that can be up to 99% (v/v) CO_2 [8] [Fig. 2].

At large, CO_2 separation costs are expected to be directly related to the purity of the waste gas stream, with more dilute CO_2 sources requiring higher energy inputs and contact areas that directly translate to increased costs.[9] As a result, the most concentrated CO_2 streams will require the least processing and can theoretically offer the best value proposition for reactive CO_2 conversion. For example, bioethanol plant effluent (~99% (v/v) CO_2) could potentially be purified at costs as low as $20–25 per tonne CO_2 while more dilute sources like power plant flue gases (10–30% (v/v) CO_2) may cost almost two to four times as much ($40–100 per tonne), and exceptionally dilute sources like air (~420 ppm) may cost almost ten times as much ($300–1000 per tonne, Fig. 2). As the capital and operational expenditures for CO_2 separation technologies can be substantial, an ideal scenario might be to avoid or limit gas feed separation in emerging CO_2 valorization processes. In-line with this idea, some have begun to test dilute sources of CO_2 such as flue gas in electrochemical and bio-electrochemical CO_2 conversion nanotechnologies but the impact of gas purity on nanomaterial performance and design has yet to be considered across studies. In this perspective, we conducted a state-of-the-art technical analysis to evaluate the impact of gas purity on CO_2 transformation in emerging electrified CO_2 conversion processes. We identify suitable nanomaterials for dilute gas conditions, analyze CO_2 conversion mechanisms at the nano-bio interface, and discuss opportunities to improve the economic viability of employing these technologies in large-scale industrial applications. Through this wide-ranging evaluation, we provide comparative life-cycle assessment and technoeconomic analysis calculations for CO_2 conversion and illuminate bottlenecks in process design and operation, guiding future nanomaterial research and development.

2. Impact of gas purity on CO_2 conversion.

2.1 Electrocatalytic CO_2 conversion nanomaterials

In electrocatalytic CO_2 conversion, an external voltage is applied across a set of electrodes, causing electrons and protons to be liberated in an oxidation reaction occurring at the anode electrode for subsequent use in the reduction of CO_2 at the cathode electrode. Typically, redox active nanomaterials are deposited on the surface of the cathode to lower activation energies and mediate the transfer of

electrons to CO_2 to produce an extensive portfolio of products. Recently, a wide range of metals,[10] 2D materials,[11] alloys,[12] metal oxides,[13] single atoms,[14] and hetero atom-doped carbon materials[15] have been used as active catalysts for the CO_2 reduction reaction (CO_2-RR) [Fig. 3]. The reduction of CO_2 to its simplest product, CO, is currently thought to occur through the following reaction steps as indicated by recent density functional theory (DFT) calculations:[16] CO_2 adsorption (i); the formation of $COOH_{abs}$ (ii, eqn (1)); the formation of CO_{abs} (iii, eqn (2)) and CO desorption from the catalyst surface (iv).

$$CO_{2(abs)} + H^+ + e^- \rightarrow COOH_{(abs)} \quad (1)$$

$$COOH_{(abs)} + e^- \rightarrow CO_{abs} + OH^- \quad (2)$$
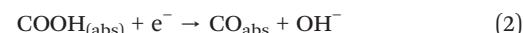
Notably, nanoparticles of noble metals such as silver have been shown to generate CO with excellent Faradaic efficiencies (FEs) approaching unity.[17] Moreover, nitrogen-doped carbon materials including N-doped mesoporous carbon,[18] graphene quantum dots,[19] and nanofibers[20] have demonstrated excellent selectivity for the CO_2-RR, owing to the high electronegativity of N-atoms that can increase the electron density of CO_2 reduction sites. In particular, single-atom decorated N-doped (Mi–N–C) materials have highly dense active sites dispersed at the atomic level that can achieve exceptional CO_2-RR rates and selectivity.[21] Likewise, single atom catalysts supported on carbon black have also achieved high FEs for CO up to 98.9% with low overpotentials.[22] Though promising, the bulk of these catalysts have exclusively been tested under high purity CO_2 gas streams (*i.e.* 99% (v/v)) and the performance of the select nanomaterials that have been tested under dilute CO_2 gas blends are yet to be compared across studies. Data was compiled from various publications that have tested dilute CO_2 blends as a feedstock for electrochemical CO_2 conversion to elucidate the state-of-the-art under these operating conditions [Fig. 4].

Rates of CO_2 conversion seem to be heavily reliant on the composition of the influent gas feedstock [Fig. 4]. For instance, when utilizing a high purity CO_2 blend of 99% (v/v), an Ag nanoparticle catalyst achieved a partial current density of 52 mA cm^{-2} compared to just 28 mA cm^{-2} when using a much more dilute CO_2 blend of 10% (v/v) [Fig. 4A]. This aligns with expected behavior, as a higher reactant concentration in the feed should lead to a higher reaction rate, and thus a higher partial current density for CO formation. Notably, the severity of the performance decline under dilute gases seems to be strongly correlated with the reactor architecture used for electrolysis. While using a flow cell fitted with gas diffusion electrodes (GDEs), the decrease in reported current densities between operating with 99% (v/v) CO_2 and 20% (v/v) CO_2 was only 25%. In comparison, a nearly 80% drop was reported when using an H-cell reactor under similar conditions [Fig. 4C]. This is likely because the triple phase boundary layer offered by GDEs allows for CO_2 to be better dispersed and utilized across the electrode
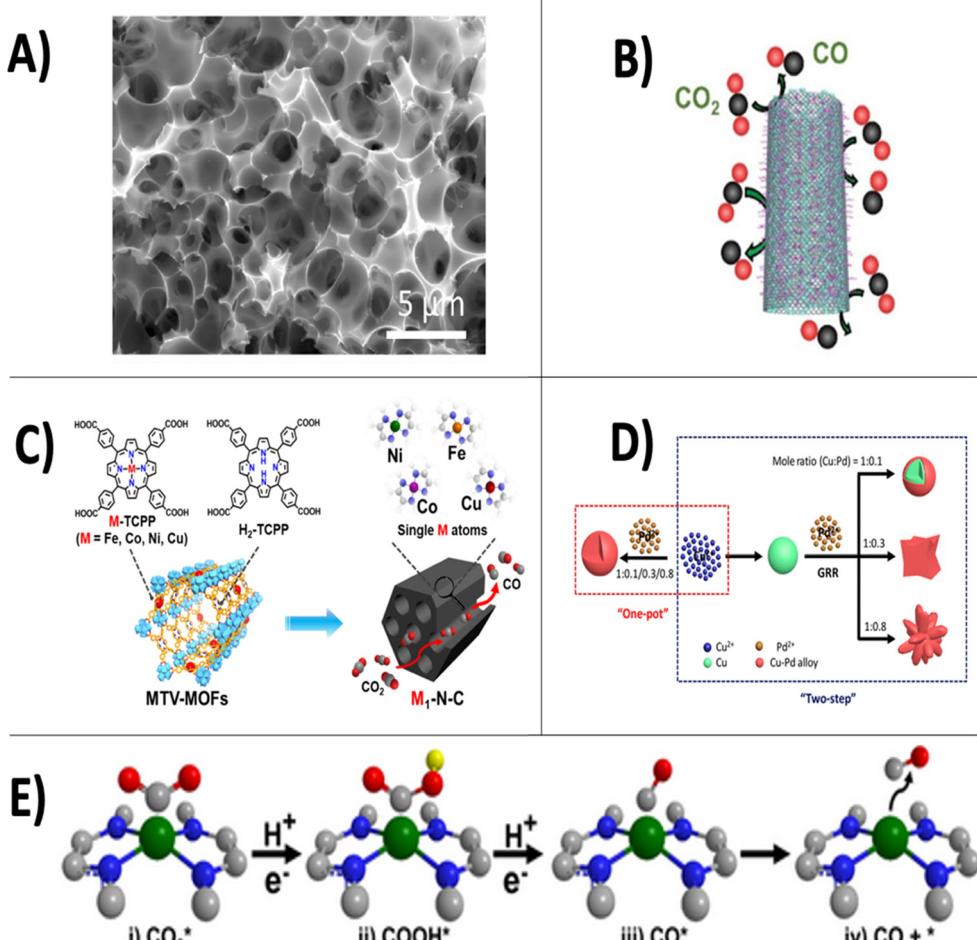
Fig. 3 Overview of state-of-the-art nanomaterials employed for electrocatalytic CO_2 reduction using dilute CO_2 gas feedstock. Transmission electron microscopy image of porous nitrogen doped carbon material from wheat flour substrate, reproduced from ref. 23 with permission of Elsevier publishers, Copyright 2017 (A). Imine-nitrogen doped carbon nanotubes used for the electrocatalytic reduction of flue gases, reproduced from ref. 24 with permission of Wiley publishers, Copyright 2021 (B). Fabrication method for single-atom decorated N-doped carbon catalysts based on multivariate metal–organic frameworks, reproduced from ref. 21 with permission of Wiley publishers, Copyright 2020 (C). Synthesis of bimetallic copper–palladium nanoalloys, reproduced from ref. 25 with permission of American Chemical Society publishers, Copyright 2018 (D). Depiction of CO_2 reduction pathway to CO using single-atom decorated N-doped carbon catalysts, reproduced from ref. 21 with permission of Wiley publishers, Copyright 2020 (E).

surface.[26] In addition, CO_2 is sparingly soluble in water, presenting kinetic challenges in H-cell reactors that rely on dissolved CO_2.[27] Similar to reactor architecture, the intrinsic properties of the electrode nanomaterials also seem to play a large role in the current densities observed for CO formation. For instance, Ni–N–C catalysts were reported to experience around a 90% drop in current density when operating in 15% (v/v) CO_2 rather than 99% (v/v) CO_2, while in a separate study comparable NCNT-NH_3 catalysts experienced just a ~60% drop in current density across similar conditions [Fig. 4B]. Though these materials are alike in composition, the disparity in their catalytic activity under dilute CO_2 conditions may stem from differences in their nano-morphology, availability of active sites, relative binding affinities for CO_2-RR intermediates, and microenvironments surrounding surface N-atoms on the carbon matrix. This highlights the importance of careful nanomaterial design in achieving high rates of CO_2 conversion.

Interestingly, the FEs (*i.e.* selectivity) of the electrocatalysts seem to be far less sensitive to the composition of the feed gas. For example, similar FEs were reported for each catalyst material when operating with 99, 20, and 15% (v/v) CO_2 as the average slope of the line of best fit across all studies was <1%. This implies that for every 1% increase in CO_2 concentration in the feed there was a near negligible 0.1% increase in average FEs for CO production with a given catalyst material [Fig. 4B]. This data is promising as FEs seem to be highly dependent on the nanomaterial properties rather than the CO_2 concentration of the feed gas. This is further illustrated by the observation that the drop in FEs across all catalysts were between 5% and 16% when operating in dilute CO_2 blends of 15% and 20% (v/v) rather than 99% (v/v) [Fig. 4D]. Altogether these relationships suggest that a high purity CO_2 feedstock may not be an absolute prerequisite for attaining high CO_2 conversion efficiencies.

This journal is © The Royal Society of Chemistry 2024

Environ. Sci.: Nano, 2024, **11**, 1770–1783 | **1773**
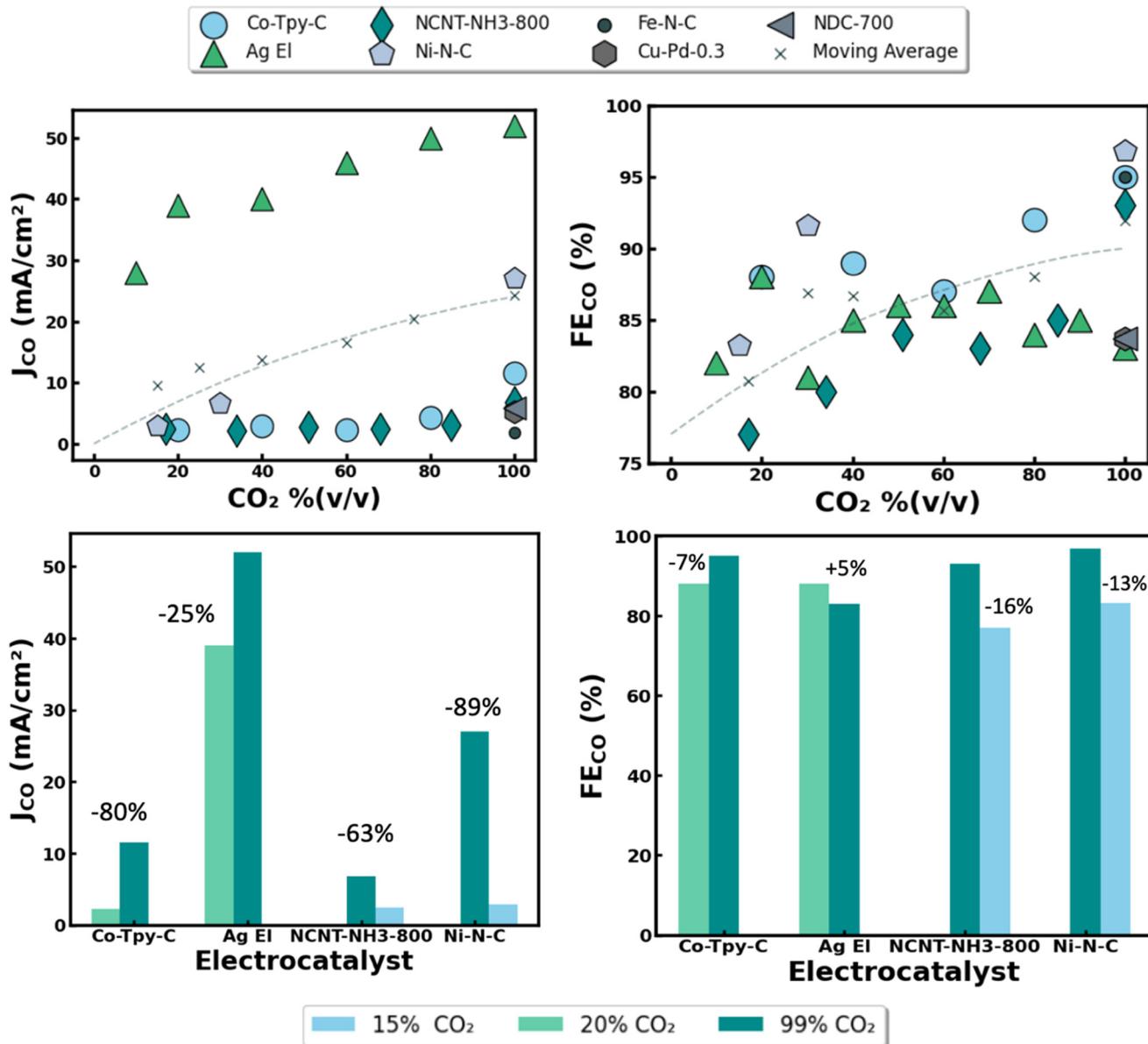
Fig. 4 Summary of reported performance metrics for abiotic electrocatalytic CO_2 conversion nanomaterials across various feedstock purity. Reported partial current density for CO formation (J_{CO}) vs. influent CO_2 concentration by percent volume, balanced with inert gas (i.e. argon). (A) Faradic efficiencies for CO formation (FE_{CO}) vs. influent CO_2 concentration used by percent volume, balanced with inert gas. (B) Detailed performance impact on current densities (C) and faradaic efficiencies (D) using different electrocatalysts and reactor designs at various influent CO_2 concentrations. Relative performance drop under dilute gas conditions listed as percentage above data bars. Electrocatalyst material abbreviations defined as follows: Co-Typ-C = cobalt terpyridine on carbon, Ag El = silver nanoparticles in electrolyzer, NCNT-NH_3-800 = imine-nitrogen-doped carbon nanotubes prepared under NH_3 at 800 °C, Ni–N–C = single atom nickel on nitrogen doped carbon. Data adapted from recent publications ref. 21, 23–25 and 34–36.

Though this data is encouraging, several challenges of operating with dilute CO_2 gas streams should be considered. These include the competitive hydrogen evolution reaction (HER) and oxygen reduction reaction (ORR) that can impact CO_2-RR selectivity as well as toxic impurities in the feed gas that can cause catalyst poisoning and deactivation. As noted in several works, low concentrations of CO_2 in the gas feed may enable greater selectivity for the HER that occurs at similar redox potentials.[21] For instance, Kim et al. (2021) recently noted that H_2 evolution sharply increased when operating an Ag catalyst in 0.1 atm CO_2 rather than a higher purity gas feed containing 1 atm CO_2.[28] Mechanistically, this is likely because the lack of surface-adsorbed CO_2 under dilute CO_2 feedstock enables active sites to be used for H_2 production rather than the CO_2-RR. Future studies may be able to address this issue by fine tuning the active sites on the nanomaterials to have a higher binding energy for *H adsorption, making the Volmer step of the HER (eqn (3)) more difficult to initiate.[29] Likewise, permselective coatings may be used at the cathode to repel

HER reactants, while allowing the passage of CO_2 to the electrode surface.

$$H^+ + e^- \rightarrow H_{(ads)} \tag{3}$$

Similar to the HER, industrial CO_2 emissions such as flue gas often contain non-innocent reactants (e.g. O_2, SO_2, or NO_X) that can divert electrons away from the CO_2-RR or cause electrode poisoning. For instance, transition metal nanocatalysts on N-doped carbon nanomaterials can readily catalyze the ORR, which may lower CO_2-RR selectivity.[30,31] In-line with this, Shi et al. (2021) noted the appearance of ORR redox peaks when conducting linear sweep voltammetry experiments in simulated flue gas (15% (v/v) CO_2, 77% (v/v) N_2 and 8% (v/v) O_2) using NCNT-NH$_3$ catalysts.[24] As such, future operations may seek to remove O_2 from feed gases prior to CO_2 conversion. Alternatively, catalysts may be redesigned to resist ORR reaction steps such as OH^- adsorption[32] but this could also destabilize CO_2-RR intermediates if not done carefully. Distinct from the ORR, Komatsu et al. (1994) also found that SO_2 can reduce CO_2-RR efficiencies when using copper-solid polymer electrolyte-based electrodes with a feed gas of 60% (v/v) CO_2 and 170 ppm SO_2.[33] The authors attributed this to corrosion of the catalyst surface, however, the reaction mechanisms for the performance drop were not further investigated. As such, additional studies are needed to systematically test the impact of common non-innocent reactants (e.g. O_2, SO_2, NO_X) on electrode poisoning as the majority of previous works have simply blended CO_2 with chemically inert gases. Overall, these experiments could provide researchers with improved understanding of catalyst deactivation modes to help future studies fine-tune the nano-morphology and surface-active sites of nanomaterials to avoid competitive reduction reactions and mitigate catalyst poisoning.

2.2 Bio-electrocatalytic CO_2 conversion nanomaterials

Microbial electrosynthesis (MES) is a bio-electrocatalytic approach to convert CO_2 and renewable electricity into value-added fuels and products. Distinct from abiotic electrochemical CO_2 reduction, a typical MES process uses chemolithoautotrophic microorganisms as the living biocatalysts to convert CO_2 into organic compounds at a solid electrode. The cathode serves as the reducing power for the microbial metabolism, providing electrons through either direct electron transfer (DET) and/or mediated electron transfer via H_2 or alternative soluble redox shuttles.[5,37] In a seminal work by Nevin et al. (2010), the researchers showed that homoacetogenic bacteria like Sporomusa ovata can produce extracellular multi-carbon products from CO_2 and water using electrons derived from the cathode.[38] Moreover, microbes such as Geobacter and Clostridium sp. have been theorized to conduct DET using conductive nanowires or c-type cytochromes to obtain electrons from the cathode.[39,40] In addition, H_2 produced via abiotic water splitting can readily be metabolized into organics at the cathode using CO_2 as the carbon source via metabolisms such as the Wood–Ljungdhal pathway (WLP).[41] Researchers have also suggested that microbes can self-produce extracellular enzymes[42] or deposit endogenous metal nanoparticles[43] onto electrodes that can catalyze the in situ production of H_2 from water, alluding to yet another route of electron transfer.

To date, an extensive portfolio of products (e.g. C2–C6 carboxylic acids, alcohols) has been demonstrated using MES, however, acetate remains the most common end-product and presents one of the most feasible options for full-scale deployment.[44] This is because the production of acetate through the WLP is one of the most energy efficient carbon fixation mechanisms as it avoids the majority of ATP-consuming reactions by combining endergonic reactions with other non-ATP consuming exergonic reactions.[45] At large, incorporating microbes as active CO_2 conversion catalysts offers several advantages over abiotic processes including 1) highly selective synthesis of large chain organics, 2) robust operational stability, 3) exceptional process flexibility across various pH, temperatures, and pressures, and 4) low operational costs owing to the self-replicating nature of microbes that avoids the need for expensive catalyst replacement (e.g. precious metals).

Contrary to these key benefits, MES processes have routinely been challenged by low production rates due to the limited conductivity and surface area of the electrodes used to culture microbes.[46] Over the last decade, researchers have tested a variety of carbonaceous, metallic, and composite carbon-metallic nanomaterials to accelerate catalytic activity at the electrode-microbial interface.[47] In general, MES cathodes must possess low CO_2 mass transfer resistance as well as high surface area, chemical stability, and biocompatibility for optimal performance. Recently, highly conductive metals such as iron,[48] nickel,[49] rubidium,[50] platinum,[51] gold,[52] and molybdenum,[53] have been tested as MES cathodes but have generally shown poor corrosion resistance in microbial media-electrolytes, leading to metal leaching into the surrounding solution that can inhibit microbial growth and metabolic activities.[6] Similar challenges have also been a concern when using metal nanomaterials (e.g. nickel nanowires,[54] Fe_2O_3[55]) deposited on carbon electrodes as MES cathodes.[56] As such, carbonaceous materials have been the most popular class of MES cathode materials owing to their high specific surface areas, excellent chemical stability, and low-cost. These include 2D planar structures such as carbon cloths[57] as well as porous 3D materials such as carbon foam,[58] felts,[59] and brushes.[60] Moreover, some have recently begun to coat carbon substrates (2D or 3D) with additional carbon nanomaterials such as graphene[7] or nanotubes[61] that can lead to higher surface areas for microbial attachment and improved electrical conductivities. For instance, cathodes made of multiwalled carbon nanotubes deposited onto reticulated vitreous carbon achieved some of the highest current densities (200 A m^{-2}) and acetate production rates (1330 g m^{-2} per day) reported to date.[62]

This journal is © The Royal Society of Chemistry 2024

Environ. Sci.: Nano, 2024, 11, 1770–1783 | 1775

Though innovations in nanomaterial design have led to significant improvements in MES production rates and scalability, the added cost of feed gas separation may drag the overall value proposition of MES technologies. Fig. 5 summarizes the performance of various MES studies that have tested dilute CO_2 feedstock as a carbon source. Distinct from abiotic catalysts, living biocatalysts can maintain similar CO_2 conversion rates and selectivity across a wide range of influent CO_2 purity [Fig. 5]. High coulombic efficiencies (CE) for acetate production were reported across the various CO_2 blends examined [Fig. 5A]. For instance, when using reticulated vitreous carbon nanotube (RVC-NT) cathodes the reported drop in CE was only ~2% when operating in 30% (v/v) CO_2 rather than the ideal 99% (v/v) CO_2 feedstock. Likewise, carbon/graphite cathodes enabled CEs of around 80–100% regardless of CO_2 purity. This partly may be because microbes can

scavenge even small quantities of CO_2 from their environments,[63,64] leading to similar metabolic efficiencies regardless of the initial amount of CO_2 that is available to them beyond a certain threshold. In addition, many of these studies used enriched cultures in combination with chemical additions (i.e. 2-bromoethanesulfonic acid) to prevent methanogenesis, which may have further enhanced CEs for acetate production via acetogenesis. Analogous to CEs, comparable current densities and production rates were also observed across the range of influent gas blends used for MES [Fig. 5B and D]. For example, RVC-NT electrodes achieved similar current densities around 35 A m^{-2}, regardless if the feed gas contained 30% or 99% (v/v) CO_2 [Fig. 5B]. In most cases, corresponding trends were also observed for the concomitant acetate production rates. For instance, similar acetate synthesis rates (ca. 11–16 g m^{-2} per day) were observed using gas diffusion (GD) electrodes
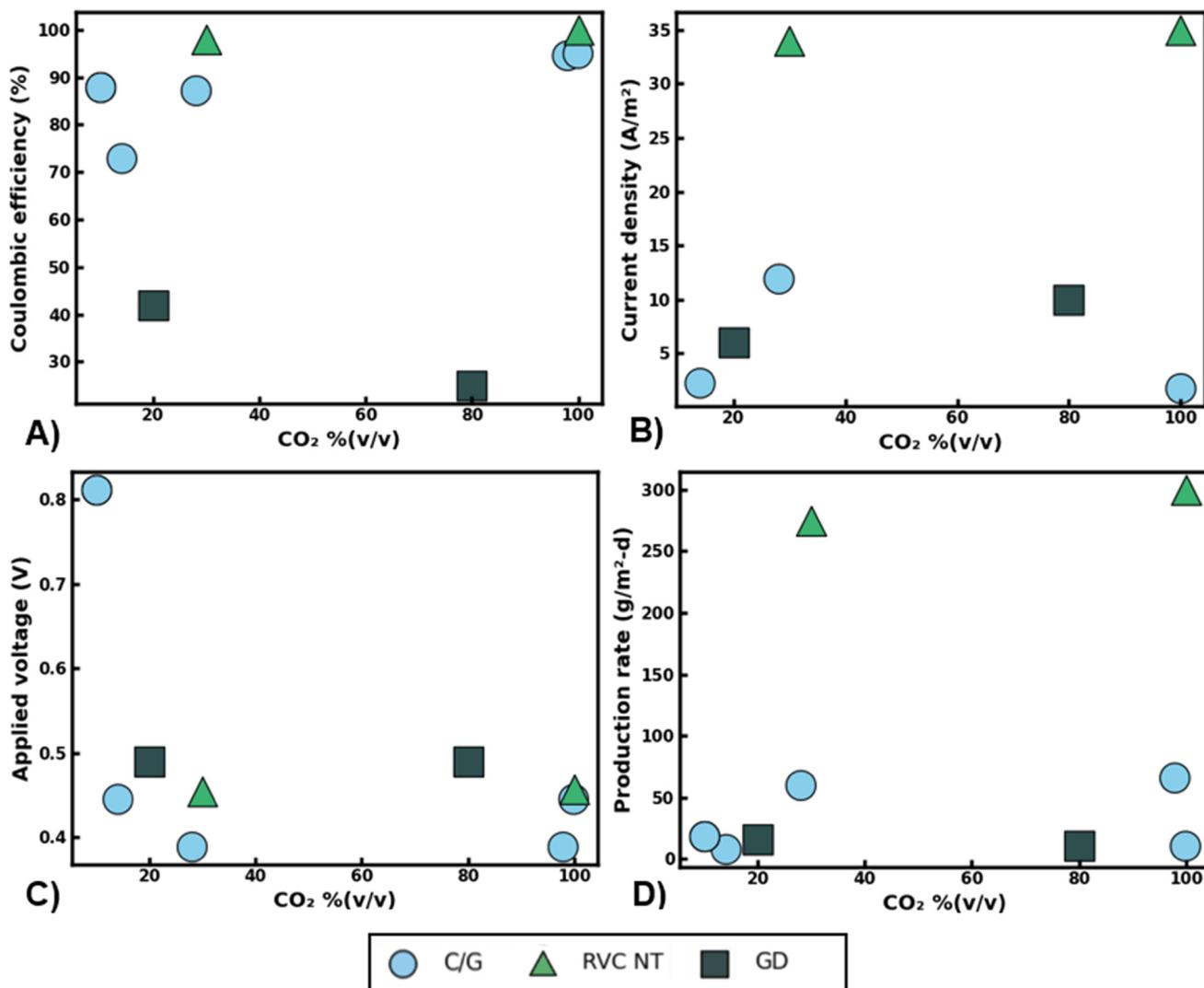
Fig. 5 Summary of reported microbial electrosynthesis performance metrics using various CO_2 gas blends and nanomaterials. Coulombic efficiency for acetate production (A) average cathodic current density (B) applied cathodic voltage versus reversible hydrogen electrode (RHE) (C) and maximum acetate production rates observed (D) versus influent CO_2 feed purity % (v/v). Cathode material acronyms: carbon/graphite (C/G), reticulated vitreous carbon nanotubes (RVC-NT), gas-diffusion (GD) electrodes. Data adapted from recent MES publications.[62,67,73–76]

with CO_2 feedstock concentrations of 20 or 80% (v/v) CO_2 [Fig. 5D]. Taken together, this indicates that CO_2 availability may not be a primary limitation in microbial electron consumption or productivity in many MES studies.

Interestingly, increasing the applied cathode voltage does not seem to lead to higher production rates under dilute CO_2 gas blends. For example, under 10% (v/v) CO_2 a carbon felt cathode operated at −0.82 V vs. RHE attained one of the lowest production rates of 19 g m^{-2} d^{-1} while a graphite plate cathode using less than half of the applied voltage (−0.39 V vs. RHE) achieved a production rate nearly three times as high (60 g m^{-2} d^{-1}, Fig. 5C). Conventionally it would be expected that the surplus of reducing power offered at higher voltages would enable more rapid production of organics. This would especially be the case in operating potentials beyond the HER. However, it is likely that the limited surface area available to the bacteria and the slow rates of extracellular electron transfer at the electrode surface were major bottlenecks to CO_2 conversion rather than a lack of sufficient reducing equivalents. This is evident as the RVC-NT cathodes that have a very high surface area (3902 m^2 m^{-3} electrode) for microbial attachment achieved 2–10 times higher average current densities than alternative cathode materials [Fig. 5B].

Though mechanisms can be difficult to discern due to a lack of standardized reporting metrics, reactor culturing techniques, and microbial communities, the data that is available so far points to the promising ability of MES processes to achieve consistent CO_2 conversion rates, electron exchange, and product selectivity, irrespective of gas feed purity. Still, several important factors must be accounted for when operating with dilute waste gases including the impact of non-innocent gaseous constituents as well as possible reactions that can compete with the CO_2-RR. In many industrial waste gases like coal power plant flue gas, O_2 can be a notable constituent ranging from 5–14% (v/v).[65] MES primarily relies on anaerobic bacteria to conduct CO_2 conversion, many of which are highly sensitive to oxygen exposure and can become inactive even at low O_2 pressures.[66] As such, the presence of O_2 in the gas feed could significantly reduce MES CO_2 conversion rates and productivities, especially when operating with pure cultures that are strict anaerobes. A potential solution could be to operate MES reactors with mixed cultures of bacteria that can leverage synergistic metabolisms for enhanced process stability. For instance, Roy et al. (2021) found that a genus of microaerophilic bacteria, Sulfurospirillum, can scavenge trace amounts of O_2 and help maintain anaerobic conditions in MES reactors.[67] However, this species can also oxidize acetate using O_2 as an electron acceptor potentially reducing CO_2-RR rates and titers. Still, if alternative organics such as aliphatic or aromatic hydrocarbons are available in the waste gas feed, bacteria such as Pseudomonas may be able to use these compounds as electron donors with the concurrent reduction of O_2 as noted by researchers when operating an MES reactor with brewery waste gas.[67] Nevertheless, more studies on this topic are needed as hydrocarbons and other volatile organic compounds could potentially be toxic to acetogenic bacteria used for CO_2 conversion. Moreover, similar microbial dynamics may impact the removal of other non-innocent compounds like SO_2 and NO_X that are routinely found in industrial waste gases like coal power plant flue gas.[68] For instance, sulfate reducing bacteria (SRB) such as Desulfovibrio desulfuricans[69] could potentially be used to remove SO_2 from MES biocathodes. However, these microbes would likely need to be supplied additional carbon and energy sources as to not impact the overall CO_2-RR rates and efficiencies towards desired products. Likewise, denitrifying bacteria could be used to remove NO_x from the MES cathode through microbial denitrification (i.e. $NO_3 \rightarrow NO_2 \rightarrow NO \rightarrow N_2O \rightarrow N_2$) but this would require strict anaerobic conditions, presenting significant compatibility issues with waste gas streams that contain high levels of oxygen.[70] Nevertheless, some have reported the existence of aerobic denitrifying bacteria such as Pseudomonas aeruginosa that may be useful for NOx removal from waste gases that contain oxygen.[71]

As engineering an optimal MES microbiome may be a complex task, a more elegant approach to improve MES compatibility with waste gas blends may be to develop new porous 3D electrode nanomaterials. As found with carbon foam, the inner pores of these structures can allow microbes to colonize areas separated from the bulk aqueous phase solution.[72] This could potentially shield microbes from non-innocent gas constituents that are transported from the dissolved bulk liquid to the electrode surface and mitigate competitive reaction pathways like the ORR. Nevertheless, these shielding effects may also decrease CO_2 diffusion to the microbes and the overall rate of CO_2 conversion. As such, new nanomaterials should be carefully designed to provide both improved microbial protection and adequate CO_2 delivery for product formation.

3. Expected costs and environmental impacts

As electrified CO_2 conversion technologies continue to mature, the cost and quality of gas feedstock will likely play a key role in the economic feasibility and sustainability of these decarbonization approaches. At a minimum, selling costs should be on-par with current fossil fuel production methods to be deemed competitive without considerable tax incentives. In the absence of new investments into CO_2 pipelines to transport purified CO_2 gas streams to distributed conversion sites, CO_2 upgrading processes will likely need to overcome substantial economic hurdles accompanying location specific separation techniques. This could ultimately lead to a trade-off between CO_2 separation costs and electricity costs for CO_2 conversion.

To better understand these relationships, production costs of various feed gas scenarios were estimated using performance metrics from recent literature [Fig. 6]. When analyzing electrocatalytic CO_2 conversion processes, representative performance values were selected for Ag

This journal is © The Royal Society of Chemistry 2024

Environ. Sci.: Nano, 2024, 11, 1770–1783 | 1777
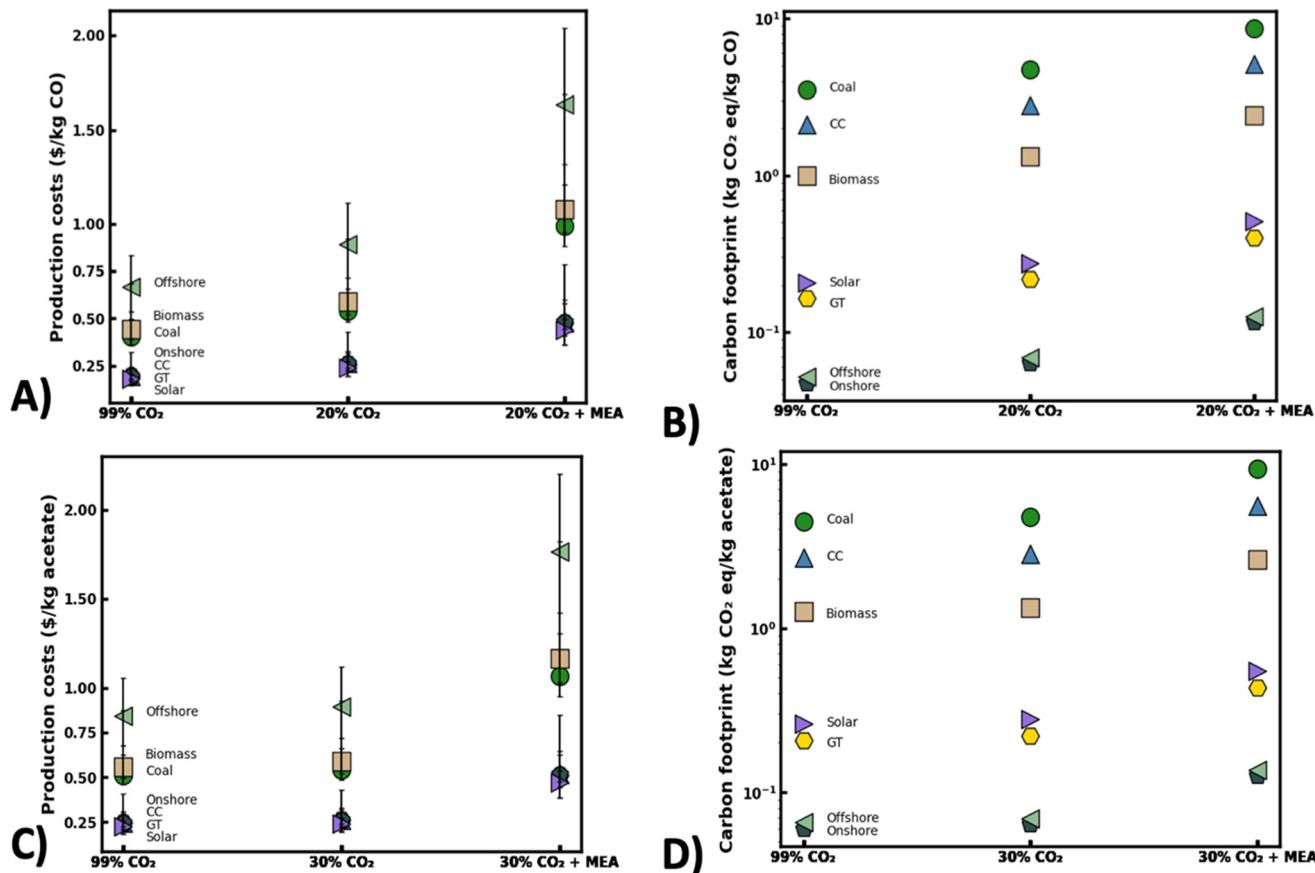
Fig. 6 Estimated production costs and carbon footprint of electrified CO_2 conversion under different waste gas feedstock scenarios. Production costs ($ per kg CO) (A) and carbon footprint (kg CO_2 eq. kg^{-1} CO formed) for electrochemical CO_2 conversion to CO (B). Production costs ($ per kg acetate) (C) and carbon footprint (kg CO_2 eq. kg^{-1} acetate formed) for bio-electrocatalytic CO_2 conversion to acetate (D). Feedstock scenarios defined as raw 20% (v/v) CO_2 purity feed without separation (20% CO_2), raw 99% (v/v) CO_2 purity feed without separation (99% CO_2), and raw 20% CO_2 (v/v) upgraded to 99% (v/v) CO_2 using standard monoethanolamine (MEA) CO_2 separation. For bio-electrocatalytic studies, 30% (v/v) CO_2 was used for dilute gas scenarios. Power source acronyms defined in Table S3.†

nanoparticle electrodes[35] as these electrocatalysts show excellent potential for scale-up owing to their high current densities and CO_2-RR selectivity. The total production costs were taken as the sum of the estimated energy costs required to produce a kg of CO_2-derived product and the accompanying separation costs to provide the associated mass of initial CO_2 feedstock [calcs. in ESI† 1.0]. Notably, capital costs for the electrolyzer and separation units were considered outside the scope of this preliminary analysis. Initial calculations were based on the scenario that a waste gas stream containing 20% (v/v) CO_2 could be used without pretreatment for CO_2 conversion [20% CO_2 scenario, Fig. 6]. This scenario is feasible as coal-fired power plants, industrial cement plants, and steel mills can frequently emit flue gases containing 15–30% (v/v) CO_2.[77,78] As such, the estimated 324 coal-fired power plants in the U.S. could potentially provide around 1200 MMT of waste CO_2 feedstock per year for CO_2 conversion.[8] In a second scenario, a high purity gas stream of 99% (v/v) CO_2 was presumed to be available for direct use without upstream separation [99% CO_2 scenario, Fig. 6]. This could be practical in CO_2 conversion sites located near

industrial bioethanol fermentation or ammonia synthesis plants that typically emit concentrated gas streams containing 95–99% (v/v) CO_2.[8] Finally, a third scenario was considered where a waste gas stream containing 20% (v/v) CO_2 might be available from an industrial point source (*e.g.* cement plant) and upgraded on-site using a monoethanolamine (MEA) CO_2 separation unit to produce a purified 99% (v/v) CO_2 feedstock for subsequent conversion [20% CO_2 + MEA, Fig. 6]. Accordingly, the integration of CO_2 capture followed by electrified CO_2 upgrading has long been envisioned as the status quo for CO_2 conversion devices.

While analyzing each scenario, energy costs were expected to be a major barrier to scalability and will likely be highly dependent on source, location, availability, and existing governmental policies/incentives.[79] As such, approximate costs of CO_2 conversion were calculated using levelized costs of energy (LCOE) from a recent U.S. Energy Information Administration (EIA) report.[80] As expected, production costs were highly sensitive to the type of energy source used [Fig. 6]. For instance, if converting a 20% (v/v) CO_2 feedstock to CO with a fossil fuel energy source like coal, estimated

production costs could be as high as $0.66 per kg CO compared to just $0.23 per kg CO when using a renewable energy source like solar photovoltaics (PV). Though price differences could be further bolstered by additional tax incentives, this highlights the tremendous opportunity to leverage low-cost renewable energy for CO_2 conversion. Notably, operating with a highly concentrated CO_2 source (*i.e.* 99% (v/v)) without upstream separation may offer even lower production costs ranging from $0.14–0.23 per kg CO [Fig. 6]. Still, these prices are 2–3 times higher than current fossil fuel-based production methods,[81] emphasizing the need to develop innovative nanomaterials that can lower energy demands (*i.e.* overpotentials) of electrochemical CO_2 conversion. Correspondingly, the 20% CO_2 (v/v) + MEA scenario yielded the highest CO production costs ranging between $0.44–1.63 per kg CO owing to expensive CO_2 separations. This suggests that purifying the 20% (v/v) CO_2 waste gas stream to a 99% (v/v) CO_2 feedstock would yield an 58% increase in CO production costs but only a 28% increase in CO production rates [Fig. 4 and 6]. Altogether, this underscores the potential benefits of avoiding expensive CO_2 separation processes and operating electrified CO_2 conversion devices with raw waste gas blends, even with existing nanomaterials.

Similar to electrocatalytic processes, acetate production costs were estimated for a pilot scale bio-electrocatalytic CO_2 conversion plant. Performance metrics were based on RVC-NT cathodes,[62] which have shown amongst the highest acetate production rates of any MES study to date and have outstanding potential for scale-up [Fig. 6]. Due to the availability of published data, this analysis was structured around a 30% (v/v) CO_2 stream rather than the 20% (v/v) CO_2 feed used for the electrocatalytic scenarios. As expected, similar trends in production costs were found with bio-electrocatalytic processes as with the abiotic processes across different energy sources. However, the production costs of the bio-electrocatalytic devices seemed to be far less impacted by gas feed composition, owing to their relatively stable performance in dilute gas streams. For instance, the average acetate production costs using on-shore wind energy were around $0.26 per kg acetate when operating with either raw 30% (v/v) or 99% (v/v) CO_2 [Fig. 6]. In contrast, the price gap was predicted to be around 34% different when operating abiotic processes under similar conditions. At large, this showcases the potential advantages of employing biocatalysts that are far less sensitive to gas feed composition for CO_2 conversion. Nevertheless, the average production costs ($0.86 per kg acetate) may be around 52% higher than current industrial acetate production methods[82] if using an MEA separation unit for gas pretreatment [30% CO_2 + MEA]. This scenario might be the case in operations that seek to maximize productivities and process stability. As such, new cathode nanomaterials are needed to improve production rates and lower energy demands in waste gas streams in order for bio-electrocatalytic processes to be competitive with existing methods at an industrial scale.

Complementing production cost estimates, the projected carbon footprint for each feedstock scenario was calculated for both electrocatalytic and bio-electrocatalytic CO_2 conversion methods [Fig. 6B and D]. Briefly, the carbon intensity of each energy source and the emission rates for a typical MEA separation unit were estimated using a current Intergovernmental Panel on Climate Change (IPCC) Report on Carbon Dioxide Capture and Storage[83] [calcs. in ESI† 2.0]. Overall, these calculations accounted for emissions from both the energy used for CO_2 conversion and power required for initial CO_2 feedstock separation while other emissions were considered outside the scope of this analysis. As expected, the carbon footprint of each process was highly dependent on the energy source used for CO_2 conversion with the most sustainable scenarios being those where renewable energy could easily be accessed. For instance, using a raw 20% (v/v) CO_2 blend for electrocatalytic CO production yielded a carbon footprint of 4.7 kg CO_2 eq. per kg CO when using coal-derived electricity *versus* just 0.27 kg CO_2 e per kg CO when using electricity generated from solar PV. Notably, the addition of a CO_2 separation unit significantly increased the estimated carbon footprint for both CO_2 conversion approaches. As an example, if using coal-derived electricity with an integrated MEA separation unit, the carbon emissions could be as high as 8.64 kg CO_2 eq. per kg CO, marking a 59% increase in emissions compared to the scenario where the separation process was omitted [*i.e.* 20% CO_2 scenario, Fig. 6]. Likewise, integration of the MEA separation unit with the bio-electrocatalytic process yielded a nearly 65% increase in emissions compared to the scenario without feedstock pretreatment. Importantly, the case where a high purity 99% (v/v) CO_2 blend could be used directly offered some of the lowest carbon footprints available. For example, using the raw 99% (v/v) CO_2 blend for acetate production with solar PV delivered an estimated carbon footprint of just 0.26 kg CO_2 eq. per kg acetate which is much lower than current petrochemical based production methods (~1 kg CO_2 eq. per kg acetate).[84] As such, the most competitive approach in terms of cost and environmental sustainability would be to use a raw 99% (v/v) CO_2 blend without feedstock separation combined with a renewable energy source like solar PV or onshore wind. Still, a scenario where renewable energy is readily available alongside a high purity CO_2 emission source may be rare and prove difficult to utilize at meaningful production scales. Accordingly, the widespread adoption of emerging carbon cycling technologies will demand new nanomaterials that cannot only improve present energy efficiencies and production rates under ideal feedstock scenarios but also enable stable CO_2 conversion using a wide range of industrial waste gas emissions.

4. Future outlook for CO_2 conversion nanomaterials

This technical review and analysis underscores the outstanding potential of waste CO_2 valorization as an economic and

This journal is © The Royal Society of Chemistry 2024

Environ. Sci.: Nano, 2024, **11**, 1770–1783 | **1779**

sustainable pathway to reduce carbon emissions. By evaluating recently published data, unique challenges faced by respective electrocatalytic and bio-electrocatalytic processes were brought to light that warrant the synthesis of innovative nanomaterials. In general, both electrocatalytic and bio-electrocatalytic methods show excellent potential for converting CO_2 into useful fuels and chemicals. However, these technologies have typically shown complementary limitations as electrocatalytic devices can generally reduce CO_2 into smaller C1 molecules (*e.g.* CO, formic acid) at high rates and efficiencies but have struggled to produce larger compounds (>C2) with high selectivity.[8] Meanwhile, bio-electrocatalytic approaches can produce a wide range of larger molecules (*e.g.* alcohols, olefins) from CO_2 with high selectivity but often suffer from slow production rates.[85] As such, a tradeoff currently exists between the high rates of electron transfer that can be achieved electrochemically and the high product selectivity that can be achieved using microbial catalysts.

Through this study, the rates of electrocatalytic CO_2-RR showed a considerable dependence on feedstock purity that was correlated with reactor architecture and electrocatalyst design. Though high selectivity can still be achieved under dilute CO_2 feedstock, new engineered nanomaterials that can attain low overpotentials and high turnover frequencies are needed to realize scalable CO_2 conversion under low CO_2 pressures. Other challenges include the presence of non-innocent compounds and particles that can lower CO_2-RR efficiencies or cause catalyst poisoning. Key approaches to address these challenges may include the development of new catalyst materials with surface active sites that are highly selective for the CO_2-RR but resistant to side reactions such as the HER or ORR. Regardless of CO_2 feedstock composition, these are highly desirable attributes and should be a strong focus of future nanomaterial studies. In addition, more work is needed to address issues stemming from catalyst poisoning by common constituents of waste gas feedstock that can be chemically active including NO_x and SO_x. Accordingly, the mechanisms for catalyst poisoning should be systematically studied with these constituents (and others) on various CO_2-RR nanomaterials to guide future catalyst design for improved waste gas compatibility. This iterative process could be accelerated using new machine learning approaches that combine DFT models with material science libraries to predict catalyst designs with desirable properties.[86] Once optimal catalysts have been identified, approaches such as permselective coatings may be applied overtop of the CO_2-RR catalysts to block impurities while allowing efficient transfer of reactants (*i.e.* CO_2) to the electrode interface. Similar methods have already been applied in seawater electrolysis using MnO_x protective layers over IrO_x catalysts.[87] Furthermore, the surface charge or electronic state of the CO_2-RR catalysts can be adjusted to repel non-innocent compounds by adding co-catalysts or polymers directly to the catalyst inks.[88] This strategy has proven effective when adding imidazolium polymers during CO_2-RR catalyst preparation to mitigate the HER.[27]

Aside from abiotic methods, bio-electrocatalytic CO_2 conversion processes seem to be able to achieve stable current densities and CO_2-RR selectivity across a wide range of feed gas purity. This performance may even translate to atmospheric CO_2 concentrations but further studies are needed to evaluate this scenario. In addition, new nanomaterials are required to improve the rates of the CO_2-RR that are currently limited by the usable surface area and electrical conductivity of the biocathodes. Additional work is also needed to assess the impact of non-innocent reactants such as oxygen that may be present in waste feed gases at significant concentrations. As microbiome engineering may be an important strategy to improve MES stability under waste gases, the identity and ecological role of individual microbial species needs to be further elucidated under these conditions. Specifically, parameters such as waste gas tolerance, CO_2 fixation pathway, and desired gene expression profile could be fed into machine learning algorithms trained on biological databases to help identify suitable microbial strains and communities for waste CO_2 valorization.[89] In combination with this approach, the development of new porous 3D electrodes that can potentially shelter microbes from harmful gases may also be useful in improving production efficiencies. These 3D porous electrodes could be used in conjunction with permselective coatings that block non-innocent compounds from entering the inner pores while allowing efficient CO_2 mass transport to the biocatalyst surfaces. Similarly, innovative cytoprotective layers that can be deposited onto the surface of individual microorganisms may also be a valuable tool to protect biocatalysts from waste gas constituents. This approach has been effective in protecting bacteria from reactive oxygen species in photocatalytic CO_2 conversion processes[90] and could easily be adapted to MES. Looking ahead, there has been an increasing focus on developing reactive CO_2 capture (RCC) processes that aim to directly convert captured CO_2 into products without an intermediate step where CO_2 is released from the initial CO_2 capture unit.[91] Though still in its infancy, RCC technologies could potentially provide new opportunities for electrified waste gas CO_2 conversion. Nevertheless, gas separations are expected to be a major economic and environmental burden to CO_2 conversion processes, across many of the most promising conversion technologies. As such, the rapid development of new highly stable and active engineered nanomaterials will be crucial in achieving scalable waste CO_2 conversion as part of a future net-zero economy.

Author contributions

J. Jack was the primary author of this work and contributed to the overall conceptualization. S. Bolzman and A. Weber conducted the initial literature review and preliminary TEA/LCA calculations with supervision from authors J. Jack and S. McCord.

1780 | *Environ. Sci.: Nano*, 2024, **11**, 1770–1783

This journal is © The Royal Society of Chemistry 2024

Conflicts of interest

The authors declare no competing financial interests associated with the writing of this article.

References

1 R. Amirbeigiarab, *et al.*, Atomic-scale surface restructuring of copper electrodes under CO2 electroreduction conditions, *Nat. Catal.*, 2023, **6**(9), 837–846.

2 G. Chen, *et al.*, Passivation of Cu nanosheet dissolution with Cu2+-containing electrolytes for selective electroreduction of CO2 to CH4, *Environ. Sci.: Nano*, 2022, **9**(9), 3312–3317.

3 X. Shi, X. Dong, Y. He, P. Yan and F. Dong, Light-induced halogen defects as dynamic active sites for CO2 photoreduction to CO with 100% selectivity, *Sci. Bull.*, 2022, **67**, 1137–1144.

4 X. Xiong, *et al.*, Selective photocatalytic CO2 reduction over Zn-based layered double hydroxides containing tri or tetravalent metals, *Sci. Bull.*, 2020, **65**, 987–994.

5 Y. Bian, *et al.*, H2 mediated mixed culture microbial electrosynthesis for high titer acetate production from CO2, *Environ. Sci. Ecotechnology*, 2024, **19**, 100324.

6 S. Zhang, *et al.*, A review of microbial electrosynthesis applied to carbon dioxide capture and conversion: The basic principles, electrode materials, and bioproducts, *J. CO2 Util.*, 2021, **51**, 101640.

7 N. Aryal, *et al.*, Enhanced microbial electrosynthesis with three-dimensional graphene functionalized cathodes fabricated via solvothermal synthesis, *Electrochim. Acta*, 2016, **217**, 117–122.

8 R. G. Grim, *et al.*, Transforming the carbon economy: Challenges and opportunities in the convergence of low-cost electricity and reductive CO2 utilization, *Energy Environ. Sci.*, 2020, **13**(2), 472–494.

9 G. Dipple, *et al.*, The Building Blocks of CDR Systems.

10 J. Rosen, *et al.*, Electrodeposited Zn dendrites with enhanced CO selectivity for electrocatalytic CO2 reduction, *ACS Catal.*, 2015, **5**(8), 4586–4591.

11 S. Gao, *et al.*, Partially oxidized atomic cobalt layers for carbon dioxide electroreduction to liquid fuel, *Nature*, 2016, **529**(7584), 68–71.

12 G. Yin, *et al.*, Selective electro-or photo-reduction of carbon dioxide to formic acid using a Cu–Zn alloy catalyst, *J. Mater. Chem. A*, 2017, **5**(24), 12113–12119.

13 B. Kumar, *et al.*, Reduced SnO2 porous nanowires with a high density of grain boundaries as catalysts for efficient electrochemical CO2-into-HCOOH conversion, *Angew. Chem., Int. Ed.*, 2017, **56**(13), 3645–3649.

14 S.-F. Hung, *et al.*, A metal-supported single-atom catalytic site enables carbon dioxide hydrogenation, *Nat. Commun.*, 2022, **13**(1), 819.

15 H. Yang, *et al.*, Composition tailoring via N and S co-doping and structure tuning by constructing hierarchical pores: metal-free catalysts for high-performance electrochemical reduction of CO2, *Angew. Chem.*, 2018, **130**(47), 15702–15706.

16 C. Guo, *et al.*, Electrochemical CO2 reduction to C1 products on single nickel/cobalt/iron-doped graphitic carbon nitride: a DFT study, *ChemSusChem*, 2019, **12**(23), 5126–5132.

17 X. Deng, *et al.*, Breaking the Limit of Size-Dependent CO2RR Selectivity in Silver Nanoparticle Electrocatalysts through Electronic Metal–Carbon Interactions, *ACS Catal.*, 2023, **13**(23), 15301–15309.

18 Y. Song, *et al.*, Metal-free nitrogen-doped mesoporous carbon for electroreduction of CO2 to ethanol, *Angew. Chem., Int. Ed.*, 2017, **56**(36), 10840–10844.

19 J. Wu, *et al.*, A metal-free electrocatalyst for carbon dioxide reduction to multi-carbon hydrocarbons and oxygenates, *Nat. Commun.*, 2016, **7**, 13869.

20 S. Liu, *et al.*, Identifying active sites of nitrogen-doped carbon materials for the CO2 reduction reaction, *Adv. Funct. Mater.*, 2018, **28**, 1800499.

21 L. Jiao, *et al.*, Single-Atom Electrocatalysts from Multivariate Metal–Organic Frameworks for Highly Selective Reduction of CO2 at Low Pressures, *Angew. Chem., Int. Ed.*, 2020, **59**(46), 20589–20595.

22 H. Yang, *et al.*, A universal ligand mediated method for large scale synthesis of transition metal single atom catalysts, *Nat. Commun.*, 2019, **10**(1), 4585.

23 F. Li, *et al.*, Porous nitrogen–doped carbon derived from biomass for electrocatalytic reduction of CO2 to CO, *Electrochim. Acta*, 2017, **245**, 561–568.

24 H. Shi, *et al.*, Imine-Nitrogen-Doped Carbon Nanotubes for the Electrocatalytic Reduction of Flue Gas CO2, *ChemElectroChem*, 2021, **8**(10), 1792–1797.

25 D. Chen, *et al.*, Tailoring the selectivity of bimetallic copper–palladium nanoalloys for electrocatalytic reduction of CO2 to CO, *ACS Appl. Energy Mater.*, 2018, **1**(2), 883–890.

26 D. Wakerley, *et al.*, Gas diffusion electrodes, reactor designs and key metrics of low-temperature CO2 electrolysers, *Nat. Energy*, 2022, **7**, 130–143.

27 J. Jack, J. Lo, B. Donohue, P.-C. Maness and Z. J. Ren, High rate CO2 valorization to organics via CO mediated silica nanoparticle enhanced fermentation, *Appl. Energy*, 2020, **279**, 115725.

28 D. Kim, *et al.*, Electrocatalytic reduction of low concentrations of CO2 gas in a membrane electrode assembly electrolyzer, *ACS Energy Lett.*, 2021, **6**(10), 3488–3495.

29 J. C. Wilson, *et al.*, Insights into solvent and surface charge effects on Volmer step kinetics on Pt (111), *Nat. Commun.*, 2023, **14**(1), 2384.

30 J. Liu, *et al.*, A "MOFs plus ZIFs" strategy toward ultrafine Co nanodots confined into superficial N-doped carbon nanowires for efficient oxygen reduction, *ACS Appl. Mater. Interfaces*, 2020, **12**(49), 54545–54552.

31 G. Zhu, *et al.*, Modulating the Electronic Structure of FeCo Nanoparticles in N-Doped Mesoporous Carbon for Efficient Oxygen Reduction Reaction, *Adv. Sci.*, 2022, **9**(15), 2200394.

32 Y. Sha, *et al.*, DFT prediction of oxygen reduction reaction on palladium–copper alloy surfaces, *ACS Catal.*, 2014, **4**(4), 1189–1197.

This journal is © The Royal Society of Chemistry 2024

Environ. Sci.: Nano, 2024, **11**, 1770–1783 | 1781

33 S. Komatsu, et al., Preparation of cu-solid polymer electrolyte composite electrodes and application to gas-phase electrochemical reduction of CO2, Electrochim. Acta, 1995, 40(6), 745–753.

34 P. Hou, et al., Well-defined single-atom cobalt catalyst for electrocatalytic flue gas CO2 reduction, Small, 2020, 16(24), 2001896.

35 B. Kim, et al., Influence of dilute feed and pH on electrochemical reduction of CO2 to CO on Ag in a continuous flow electrolyzer, Electrochim. Acta, 2015, 166, 271–276.

36 S. Wu, et al., Highly exposed atomic Fe–N active sites within carbon nanorods towards electrocatalytic reduction of CO2 to CO, Electrochim. Acta, 2020, 340, 135930.

37 X. Zhu, et al., Syngas mediated microbial electrosynthesis for CO2 to acetate conversion using Clostridium ljungdahlii, Resour., Conserv. Recycl., 2022, 184, 106395.

38 K. P. Nevin, et al., Microbial electrosynthesis: Feeding microbes electricity to convert carbon dioxide and water to multicarbon extracellular organic compounds, mBio, 2010, 1, e00103-10.

39 K. P. Nevin, et al., Electrosynthesis of organic compounds from carbon dioxide is catalyzed by a diversity of acetogenic microorganisms, Appl. Environ. Microbiol., 2011, 77(9), 2882–2886.

40 S. T. Boto, et al., Microbial electrosynthesis with Clostridium ljungdahlii benefits from hydrogen electron mediation and permits a greater variety of products, Green Chem., 2023, 25(11), 4375–4386.

41 J. Jack, J. Lo, P.-C. Maness and Z. J. Ren, Directing Clostridium ljungdahlii fermentation products via hydrogen to carbon monoxide ratio in syngas, Biomass Bioenergy, 2019, 124, 95–101.

42 J. S. Deutzmann, M. Sahin and A. M. Spormann, Extracellular enzymes facilitate electron uptake in biocorrosion and bioelectrosynthesis, mBio, 2015, 6(2), e00496-15.

43 E. V. LaBelle, et al., Influence of acidic pH on hydrogen and acetate production by an electrosynthetic microbiome, PLoS One, 2014, 9(10), e109935.

44 P. Bakonyi, et al., CO2-refinery through microbial electrosynthesis (MES): A concise review on design, operation, biocatalysts and perspectives, J. CO2 Util., 2023, 67, 102348.

45 S. W. Ragsdale and E. Pierce, Acetogenesis and the Wood–Ljungdahl pathway of CO2 fixation, Biochim. Biophys. Acta, Proteins Proteomics, 2008, 1784(12), 1873–1898.

46 J. Jack, et al., Anode co-valorization for scalable and sustainable electrolysis, Green Chem., 2021, 23(20), 7917–7936.

47 B. Bian, et al., Microbial electrosynthesis from CO2: Challenges, opportunities and perspectives in the context of circular bioeconomy, Bioresour. Technol., 2020, 302, 122863.

48 C. M. Dykstra and S. G. Pavlostathis, Zero-valent iron enhances biocathodic carbon dioxide reduction to methane, Environ. Sci. Technol., 2017, 51(21), 12956–12964.

49 M. F. Alqahtani, et al., Porous hollow fiber nickel electrodes for effective supply and reduction of carbon dioxide to methane through microbial electrosynthesis, Adv. Funct. Mater., 2018, 28(43), 1804860.

50 S. Das, S. Das and M. M. Ghangrekar, Application of TiO2 and Rh as cathode catalyst to boost the microbial electrosynthesis of organic compounds through CO2 sequestration, Process Biochem., 2021, 101, 237–246.

51 A. Nandy, et al., Comparative evaluation of coated and non-coated carbon electrodes in a microbial fuel cell for treatment of municipal sludge, Energies, 2019, 12(6), 1034.

52 M. Sun, et al., A gold-sputtered carbon paper as an anode for improved electricity generation from a microbial fuel cell inoculated with Shewanella oneidensis MR-1, Biosens. Bioelectron., 2010, 26(2), 338–343.

53 M. Siegert, et al., Comparison of nonprecious metal cathode materials for methane production by electromethanogenesis, ACS Sustainable Chem. Eng., 2014, 2(4), 910–917.

54 C. Liu, et al., Nanowire–bacteria hybrids for unassisted solar carbon dioxide fixation to value-added chemicals, Nano Lett., 2015, 15(5), 3634–3639.

55 M. Cui, et al., Three-dimensional hierarchical metal oxide–carbon electrode materials for highly efficient microbial electrosynthesis, Sustainable Energy Fuels, 2017, 1(5), 1171–1176.

56 D. Thatikayala and B. Min, Copper ferrite supported reduced graphene oxide as cathode materials to enhance microbial electrosynthesis of volatile fatty acids from CO2, Sci. Total Environ., 2021, 768, 144477.

57 L. Yu, et al., Thermophilic Moorella thermoautotrophica-immobilized cathode enhanced microbial electrosynthesis of acetate and formate from CO2, Bioelectrochemistry, 2017, 117, 23–28.

58 E. V. LaBelle and H. D. May, Energy efficiency and productivity enhancement of microbial electrosynthesis of acetate, Front. Microbiol., 2017, 8, 756.

59 H.-Y. Yang, et al., Redox mediator-modified biocathode enables highly efficient microbial electro-synthesis of methane from carbon dioxide, Appl. Energy, 2020, 274, 115292.

60 H. T. H. Nguyen and B. Min, Using multiple carbon brush cathode in a novel tubular photosynthetic microbial fuel cell for enhancing bioenergy generation and advanced wastewater treatment, Bioresour. Technol., 2020, 316, 123928.

61 L. Jourdin, et al., A novel carbon nanotube modified scaffold as an efficient biocathode material for improved microbial electrosynthesis, J. Mater. Chem. A, 2014, 2(32), 13093–13102.

62 L. Jourdin, et al., Bringing high-rate, CO2-based microbial electrosynthesis closer to practical implementation through improved electrode design and operating conditions, Environ. Sci. Technol., 2016, 50(4), 1982–1989.

63 E. N. Frolov, et al., Obligate autotrophy at the thermodynamic limit of life in a new acetogenic bacterium, Front. Microbiol., 2023, 14, 1185739.

1782 | Environ. Sci.: Nano, 2024, 11, 1770–1783

This journal is © The Royal Society of Chemistry 2024

64 S. Barik, et al., Biological production of ethanol from coal synthesis gas, Bioprocess. Biotreat. Coal, 2017, 131–154.

65 E. David, et al., Exhaust gas treatment technologies for pollutant emission abatement from fossil fuel power plants, WIT Trans. Ecol. Environ., 2007, 102, DOI: 10.2495/SDP070882.

66 A. R. Oliveira, et al., An allosteric redox switch involved in oxygen protection in a CO2 reductase, Nat. Chem. Biol., 2024, 20(1), 111–119.

67 M. Roy, et al., Direct utilization of industrial carbon dioxide with low impurities for acetate production via microbial electrosynthesis, Bioresour. Technol., 2021, 320, 124289.

68 C. Oberschelp, et al., Global emission hotspots of coal power generation, Nat. Sustain., 2019, 2(2), 113–121.

69 J. Lin, et al., Continuous desulfurization and bacterial community structure of an integrated bioreactor developed to treat SO2 from a gas stream, J. Environ. Sci., 2015, 37, 130–138.

70 T. Ma, et al., Simultaneous denitrification and phosphorus removal by Agrobacterium sp. LAD9 under varying oxygen concentration, Appl. Microbiol. Biotechnol., 2016, 100, 3337–3346.

71 M. Zheng, et al., Potential application of aerobic denitrifying bacterium Pseudomonas aeruginosa PCN-2 in nitrogen oxides (NOx) removal from flue gas, J. Hazard. Mater., 2016, 318, 571–578.

72 L. Jourdin and T. Burdyny, Microbial electrosynthesis: where do we go from here?, Trends Biotechnol., 2021, 39(4), 359–369.

73 S. Bajracharya, et al., Application of gas diffusion biocathode in microbial electrosynthesis from carbon dioxide, Environ. Sci. Pollut. Res., 2016, 23, 22292–22308.

74 S. A. Patil, et al., Selective enrichment establishes a stable performing community for microbial electrosynthesis of acetate from CO2, Environ. Sci. Technol., 2015, 49(14), 8833–8843.

75 L. Rovira-Alsina, M. Dolors Balaguer and S. Puig, Transition roadmap for thermophilic carbon dioxide microbial electrosynthesis: Testing with real exhaust gases and operational control for a scalable design, Bioresour. Technol., 2022, 365, 128161.

76 M. Roy, S. Yadav and S. A. Patil, Biogas upgradation through CO2 conversion into acetic acid via microbial electrosynthesis, Front. Energy Res., 2021, 9, 759678.

77 R. J. Barla, S. Raghuvanshi and S. Gupta, Process integration for the biodiesel production from biomitigation of flue gases, Waste and Biodiesel: Feedstocks and Precursors for Catalysts, 2022, DOI: 10.1016/B978-0-12-823958-2.00007-0.

78 R. W. Baker, et al., CO2 capture from cement plants and steel mills using membranes, Ind. Eng. Chem. Res., 2018, 57(47), 15963–15970.

79 U.S. Energy Information Agency, Annual Energy Outlook 2020 with projections to 2050, Annual Energy Outlook 2019 with projections to 2050, 2019, vol. 44.

80 U.S. Energy Information Administration (EIA, Levelized Cost and Levelized Avoided Cost of New Generation Resources in the Annual Energy Outlook 2020, U.S. EIA, 2020.

81 S. Y. Chae, et al., A perspective on practical solar to carbon monoxide production devices with economic evaluation, Sustainable Energy Fuels, 2020, 4(1), 199–212.

82 X. Christodoulou and S. B. Velasquez-Orta, Microbial electrosynthesis and anaerobic fermentation: an economic evaluation for acetic acid production from CO2 and CO, Environ. Sci. Technol., 2016, 50(20), 11234–11242.

83 P. Mathieu, The IPCC special report on carbon dioxide capture and storage, in ECOS 2006 - Proceedings of the 19th International Conference on Efficiency, Cost, Optimization, Simulation and Environmental Impact of Energy Systems, 2006.

84 E. Budsberg, et al., Production routes to bio-acetic acid: life cycle assessment, Biotechnol. Biofuels, 2020, 13, 1–15.

85 J. Jack, H. Fu, A. Leininger, T. K. Hyster and Z. J. Ren, Cell-free CO2 valorization to C6 pharmaceutical precursors via a novel electro-enzymatic process, ACS Sustainable Chem. Eng., 2022, 10, 4114–4121.

86 D. H. Mok, et al., Data-driven discovery of electrocatalysts for CO2 reduction using active motifs-based machine learning, Nat. Commun., 2023, 14(1), 7303.

87 J. G. Vos, et al., MnOx/IrOx as selective oxygen evolution electrocatalyst in acidic chloride solution, J. Am. Chem. Soc., 2018, 140(32), 10270–10281.

88 R. B. Kutz, et al., Sustainion imidazolium-functionalized polymers for carbon dioxide electrolysis, Energy Technol., 2017, 5(6), 929–936.

89 R. Hernández Medina, et al., Machine learning and deep learning applications in microbiome research, ISME Commun., 2022, 2(1), 98.

90 S. Cestellos-Blanco, et al., Photosynthetic semiconductor biohybrids for solar-driven biocatalysis, Nat. Catal., 2020, 3(3), 245–255.

91 R. E. Siegel, S. Pattanayak and L. A. Berben, Reactive capture of CO2: opportunities and challenges, ACS Catal., 2022, 13(1), 766–784.

This journal is © The Royal Society of Chemistry 2024

Environ. Sci.: Nano, 2024, 11, 1770–1783 | 1783